



Short communication

Enhancement of anodic oxidation of formic acid on palladium decorated Pt/C catalyst

Yan Ni Wu^{a,b}, Shi Jun Liao^{a,*}, Yun Lan Su^c, Jian Huang Zeng^a, Dai Dang^a^a School of Chemistry and Chemical Engineering, South China University of Technology, Wushan, Guangzhou 510641, China^b School of Chemistry and Chemical Engineering, Zhao Qing University, Zhao Qing 526061, China^c Institute of Chemistry, Chinese Academy of Sciences, Beijing 100191, China

ARTICLE INFO

Article history:

Received 25 March 2010

Received in revised form 17 April 2010

Accepted 19 April 2010

Available online 24 April 2010

Keywords:

Catalyst

Colloidal approach

Formic acid oxidation

Pt@Pd/C

ABSTRACT

A palladium decorated Pt/C catalyst, Pt@Pd/C, is prepared by a colloidal approach with a small amount of platinum as core. It is found that the catalyst shows excellent activity towards anodic oxidation of formic acid at room temperature and its activity is 60% higher than that of Pd/C. Decoration of palladium shell on the platinum core is supported by XPS results. Due to the use of platinum as core, active components are dispersed very well and the particle sizes are smaller than those of Pd/C. The cyclic voltammetry measurement clearly shows synthetic electro-oxidation effects of formic acid on Pt@Pd/C. It is speculated that the high performance of Pt@Pd/C may result from the unique core-shell structure and synergistic effect of Pt and Pd at the interface. The preparation method for Pt@Pd/C reported in this work will provide additional options for the design of catalysts for direct formic acid fuel cell (DFAFC).

© 2010 Elsevier B.V. All rights reserved.

1. Introduction

Direct formic acid fuel cell (DFAFC) has attracted much attention due to its high theoretical open circuit potential (1.45 V) and low fuel crossover relative to direct methanol fuel cell [1,2]. It has been reported that there are two types of reaction mechanism for formic acid electro-oxidation, namely “direct pathway mechanism” and “dual pathway mechanism (or CO pathway mechanism)” [3]. It is desirable for formic acid electro-oxidation to go through “direct pathway” mechanism since this reaction pathway involves no significant CO poisoning.

Pd or Pd-based catalysts were found to possess better performances towards the anodic oxidation of formic acid in DFAFCs compared with Pt or Pt-based catalysts [4,5]. The superior performance of Pd-based catalyst to Pt-based catalyst is due to its direct oxidation pathway, which produces no CO intermediates [6,7]. However, the formic acid oxidation activity on monometallic Pd catalyst is still insufficient due to either the oxidation of Pd surface or the poisoning adsorption of some non-CO organic species [8,9]. Moreover, monometallic Pd can hardly be dispersed on carbon supports whatever synthesis methods are used. Good dispersion of Pt on carbon supports, however, can easily be achieved by conventional preparation techniques. Modifications on monometallic Pd catalysts deem to be necessary for obtaining more sufficient catalysts for formic acid oxidation.

There are several strategies to improve the performance of catalysts such as the use of different preparation methods [10–12], formation of alloyed catalysts (PtPb [13], Pt₄Mo [14], PdIr [8], PtOs [15], PdSn [16], PdCo [17]) and construction of hollow structures [3]. The addition of a second element either through alloying or other architecture to Pd could lead to appropriate modification of electronic and/or structural properties of Pd surface.

It is generally accepted that Pd exhibits good activity for formic acid oxidation and provides a synergistic electronic effect to Pt as well. Appropriate construction of Pt and Pd could theoretically build catalysts that are favorable for formic acid oxidation via “direct pathway” [1]. In fact, extensive studies have been made on PtPd alloyed catalyst for formic acid oxidation [18,19]. Although positive results have been reported, the catalytic activity enhancement on PtPd alloyed catalysts is somewhat not too encouraging.

Recently, core-shell nano-structured catalysts have been prepared for electro-oxidation of small organic molecules such as Au@Pt for methanol [20] and Au@Pd for formic acid [21]. The core element could promote surface oxidation (shell element) through intimate core-shell interaction leading to easier removal of CO intermediates on shell. Unfortunately, the gold core used in the reported work is inert to both methanol and formic acid oxidation. Moreover, the particle sizes synthesized in the previously reported work are not small at all (10 nm for Au@Pt [20] and 7 nm for Au@Pd [21]), thus negating the merits of core-shell structure. It is against this background we designed a facile and efficient two stage organic colloidal method to synthesize Pd coated Pt catalyst (i.e. Pt@Pd/C) for formic acid electro-oxidation. Firstly, the introduction of easily dispersed Pt as core could sufficiently improve dispersion of Pd.

* Corresponding author. Tel.: +86 20 8711 3586; fax: +86 20 8711 3586.

E-mail address: chsjliao@scut.edu.cn (S.J. Liao).

Secondly, the preparation method of Pt@Pd/C leads to Pd islands selectively on pre-formed Pt surface, which favors synergetic catalytic effects between Pt and Pd. Thirdly, both Pt and Pd elements are active for formic acid oxidation in Pt@Pd/C catalysts and the particle sizes are sufficiently small, around 4 nm. Pd is used as a shell material since it catalyzes formic acid oxidation better than Pt does. Compared with monometallic Pd/C and Pt/C catalysts with same metal loadings, Pt@Pd/C catalyst synthesized in this work displayed remarkable catalytic activity toward formic acid oxidation at room temperature.

2. Experimental

Pt/C catalyst was prepared by an organic colloid method and the detailed preparation method has been described in a previous paper [22]. Briefly, hexachloroplatinate acid and sodium citrate were dissolved in ethylene glycol (EG) to form a mixture and then stirred for 30 min. Pre-treated Vulcan XC-72 carbon black (Carbot Corp., BET: $237 \text{ m}^2 \text{ g}^{-1}$, denoted as C) was then added to the mixture under stirring. The pH of the solution was adjusted to >10 by drop-wise addition of 5 wt% KOH in EG solution. The mixture was then placed into a Teflon[®]-lined autoclave and conditioned at 160°C for 8 h, followed by filtering, washing and vacuum drying at 90°C . Pt@Pd/C catalyst was prepared by depositing a shell palladium layer (using PdCl_2 as precursor) on the surface of the Pt/C following similar approach used in the preparation of Pt/C. Monometallic Pd/C and Pt/C catalysts were similarly prepared for a fair comparison. The total metal loading was kept at 20 wt% for all the catalysts and the atomic ratio of Pd:Pt was 5.5:1 for Pt@Pd/C catalyst. It should be noted that the platinum core amount used is very small in this work.

Morphology of the catalysts was observed using scanning transmission electron microscopy (STEM, Hitachi 2000 STEM) operating at 200 kV. X-ray diffraction (XRD) patterns were recorded on a Shimadzu XD-3A (Japan) X-ray diffractometer using $\text{Cu-K}\alpha$ radiation. The tube voltage and current was maintained at 35 kV and 30 mA respectively. Diffraction patterns were collected from 20° to 80° at a scan rate of 4 min^{-1} and a step size of 0.01. All XRD results were analyzed using Jada 7.5 software from Material Data Inc. X-ray photoelectron spectroscopy (XPS) measurement was carried out on a Perkin Elmer PHI1600 system (PerkinElmer, USA) using a single $\text{Mg-K}\alpha$ radiation source operating at 300 W and 15 kV.

The catalyst performance was evaluated by cyclic voltammetry (CV) using a three electrode cell collected with an IM6e electrochemical workstation (Zahner, Germany) at room temperature. Pt gauze and an Ag/AgCl (sat.) electrode were used as the counter and the reference electrodes respectively. All the potentials reported in this work are referenced to Ag/AgCl (sat.) electrode. The measurements were performed in an electrolyte of 0.5 M H_2SO_4 or 0.5 M $\text{H}_2\text{SO}_4 + 2.0 \text{ M HCOOH}$ in a potential range from -0.2 V to 1.0 V for collection of electrochemical performance. $4 \mu\text{L}$ of the dispersion was pipetted onto a 5 mm diameter glassy carbon disk electrode to form a catalyst layer. The Pd or Pt loading of Pd/C or Pt/C on the electrode surface was 0.005 mg whereas the Pd loading for Pt@Pd/C catalyst was 0.003 mg.

3. Results and discussion

Fig. 1 shows the XRD patterns of Pt/C, Pd/C and Pt@Pd/C catalysts. For all catalysts, the peak at 24.71° is characteristic of carbon support. The strong diffraction peaks at 2θ of 40.04° , 46.23° , 67.76° are characteristics of face-centered cubic (f.c.c) Pt/C, whereas peaks at 39.99° , 46.50° and 68.17° can be attributed to f.c.c Pd/C. Pt@Pd/C displays sharper diffraction peaks, which indicates bigger particle size due to the decoration of palladium on the surface of small par-

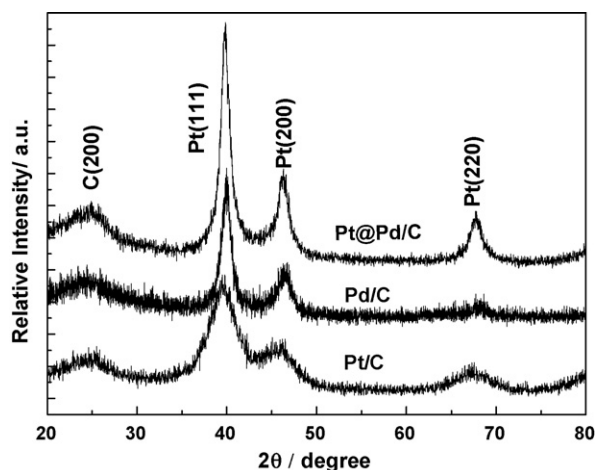


Fig. 1. XRD patterns of Pt/C, Pd/C and Pt@Pd/C catalysts.

ticles of platinum. Since the lattice mismatch of Pt and Pd is very small (0.7%), core-shell structure or alloy structure can hardly be differentiated by the XRD pattern of Pt@Pd/C catalyst. The particle size estimated by the Jada software for Pt@Pd/C, Pd/C and Pt/C catalyst was ca. 4.1 nm, 3.5 nm and 2.1 nm respectively, it is clearly that the thickness of Pd shell is ca. 1 nm. Assuming that the Pt core particle size is 2.0 nm and that the coverage of Pd layer on Pt is compact, a quick calculation would yield a thickness of Pd shell of 0.9 nm, which is quite consistent to the experimental value.

Furthermore, the XRD determined surface areas (S_{XRD}), estimated from formula $S = 6000/r.d$ [23], for Pt@Pd/C, Pt/C and Pd/C are $108.5 \text{ m}^2 \text{ g}^{-1}$, $133.2 \text{ m}^2 \text{ g}^{-1}$ and $142.6 \text{ m}^2 \text{ g}^{-1}$ respectively.

XPS has been widely used to study the surface elemental composition of nanoparticles, especially the core-shell nanoparticles with a diameter from 2 nm to 10 nm. The atomic ratio of Pd:Pt for Pt@Pd/C is 6.1:1, which is slightly higher than that of the nominal ratio of 5.5:1, indicating a Pd rich surface. The peak position for Pt(0) at 4f 5/2 is 71.11 eV and 71.07 eV for Pt/C and Pt@Pd/C whereas the peak position for Pd(0) at 3d 5/2 for Pd/C and Pt@Pd/C is 335.26 eV and 335.37 eV respectively. Since the peak position of Pt in Pt/C and Pt@Pd/C and the peak position of Pd in Pd/C and Pt@Pd/C displayed no observable difference, figures for peak deconvolution of Pt and Pd in the catalysts are not given in this work. The un-affected XPS analysis results for Pt@Pd/C relative to Pt/C and Pd/C may suggest the formation of core-shell structure since shifts of binding energies were often found in alloyed catalysts due to electron pulling or donation effects. Furthermore, it is reasonable that Pd would decorate on the Pt particles selectively other than formation of independent Pd particles on the surface of carbon.

Fig. 2 represents the TEM images of the catalysts. It can be seen that the nanoparticles are fairly well dispersed on the carbon surface for Pt/C whereas poor dispersion can be easily seen on Pd/C catalyst. The dispersion of Pt@Pd/C is better than that for Pd/C although less desirable than that of Pt/C. TEM observation confirmed that the introduction of easily dispersed Pt as seed improved dispersion of Pd. The average particle size for Pt/C, Pd/C and Pt@Pd/C is 2.0 nm, 3.8 nm and 4.2 nm respectively, which is in fairly good agreement with XRD analysis. Unfortunately, it is difficult to observe core-shell structure from TEM either due to the lack of contrast between Pt and Pd. High resolution TEM images, also failed to give confirmed evidence for the core-shell structure of Pt@Pd. The larger particle size of Pt@Pd/C relative to that of Pd/C may reflect the decoration of Pd on the Pt core due to the growth of Pd on Pt.

Cyclic voltammetry is generally regarded as a surface sensitive technique that detects electrochemical properties of surface

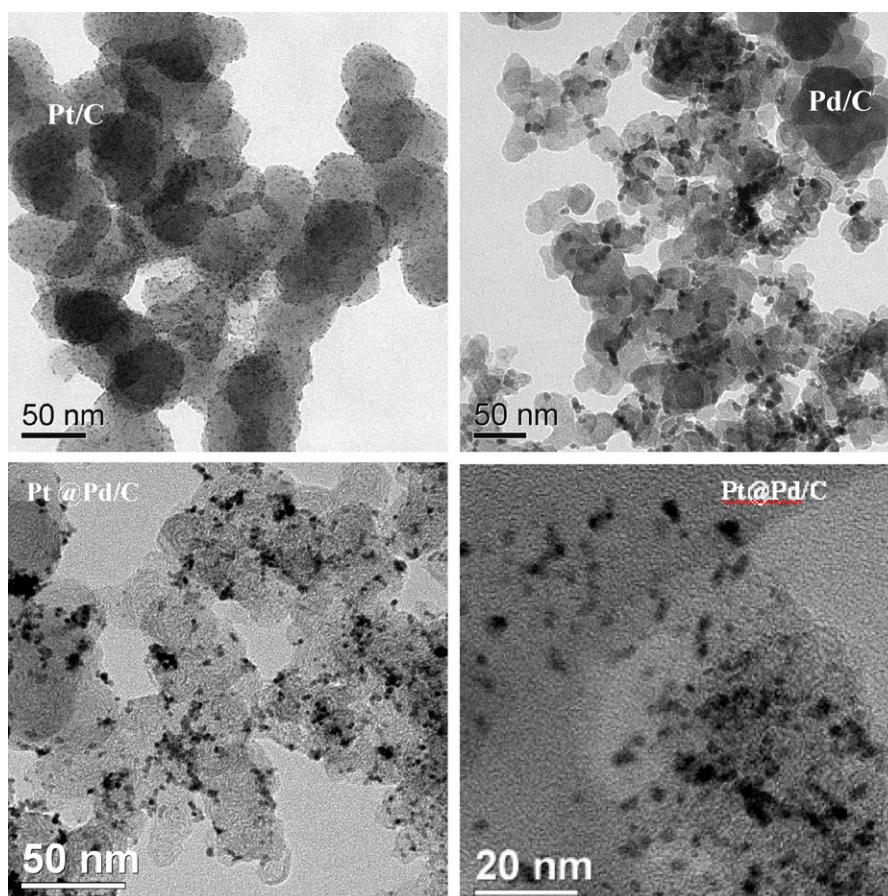


Fig. 2. TEM images of (a) Pt/C, (b) Pd/C and (c and d) Pt@Pd/C catalysts.

atoms rather than bulk atoms. Fig. 3 displays the cyclic voltammograms of Pt/C, Pd/C and Pt@Pd/C catalysts measured in N_2 -purged 0.5 M H_2SO_4 electrolyte at room temperature. It can be observed that Pt/C showed well-defined hydrogen adsorption/desorption peaks in the region of -0.2 V to 0.1 V, whereas Pd/C displayed escalating hydrogen adsorption/desorption current at around -0.1 V. The feature of Pt@Pd/C catalyst demonstrated both the characteristics of Pd/C and Pt/C. The electrochemical active surface area (ECSA) for the catalysts could be estimated from the integrated charge of the hydrogen adsorption region of the cyclic voltammograms

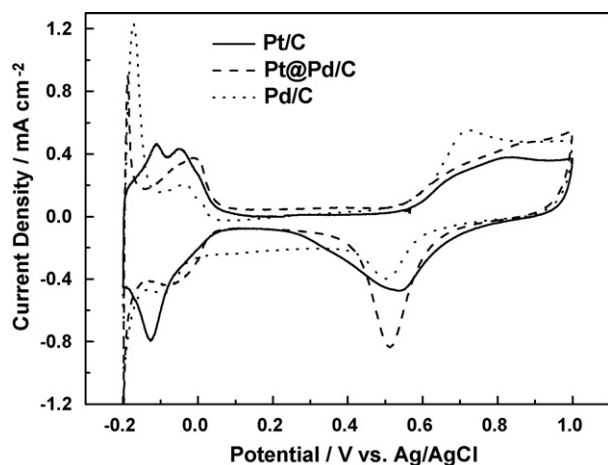


Fig. 3. Cyclic voltammograms of Pt/C, Pd/C and Pt@Pd/C catalyst electrodes measured in N_2 -purged 0.5 M H_2SO_4 electrolyte at room temperature and with a sweep rate of 20 mV s^{-1} .

[24]. The ECSA are $156.5 \text{ m}^2 \text{ g}^{-1}$, $198.0 \text{ m}^2 \text{ g}^{-1}$ and $208.2 \text{ m}^2 \text{ g}^{-1}$ for Pt@Pd/C, Pt/C and Pd/C, following the same trend as that of the S_{XRD} results, and supporting the suggestion that most palladium are decorated on the platinum core, but not reduced as independent particles. It should be noted that due to the hydrogen storage of Pd, the ECSA for Pt@Pd/C and Pd/C may be overestimated. In the preparation of Pt@Pd/C, Pt/C is prepared firstly and the active sites of carbon support are mainly occupied by Pt nanoparticles. Consequently the addition of $PdCl_2$ and the reduction of Pd^{2+} largely occurred on the pre-formed Pt surfaces leaving only occasionally isolated Pd nanoparticles. As a combined result, the CV feature of Pt@Pd/C possesses both characteristics of Pt/C and Pd/C. It should be noted that Pd oxidation can be clearly observed on Pd/C in the potential range of 0.6 – 0.8 V in the positive sweep. In contrast, the oxidation of Pd on Pt@Pd/C is almost completely suppressed. It is postulated that the remarkable activity enhancement should be related to the core-shell structure and the synergistic effect of Pt and Pd at the interface, although the reasons for the improved performance of Pt@Pd/C are not fully understood and further work is still in progress to collect additional information relevant to this phenomenon. Despite this, the method of core-shell construction of Pt-Pd used in this work is promising for applications in direct formic acid oxidation fuel cells.

Fig. 4 shows the comparison of cyclic voltammograms for catalysts Pt/C, Pd/C and Pt@Pd/C in a formic acid solution. It is found that the Pt@Pd/C shows extra high performance towards formic acid oxidation although the amount of Pt core used is very small. In the forward scan, the potential of the main oxidation peak for Pt@Pd/C is at 0.08 V, 140 mV negative to that of Pd/C (0.22 V), an indication of enhanced activity for formic acid oxidation. For Pt@Pd/C catalyst, the anodic oxidation peak was at 0.08 V, which falls within the

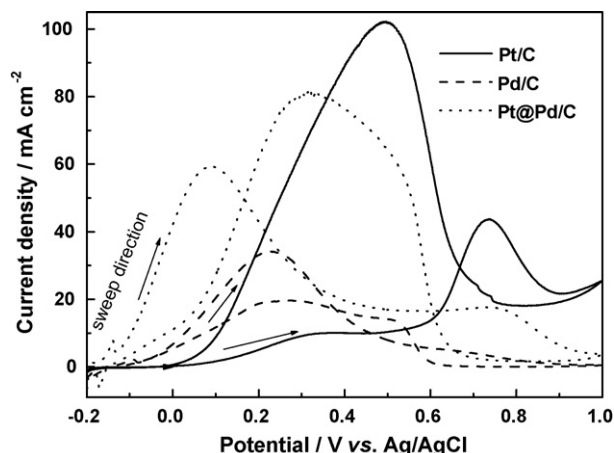


Fig. 4. Cyclic voltammograms of Pt/C, Pd/C and Pt@Pd/C catalysts in 2 M HCOOH + 0.5 M H₂SO₄ solution at a sweep rate of 10 mV s⁻¹.

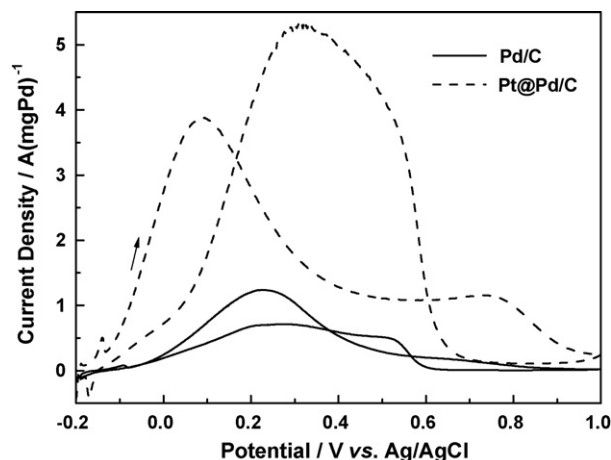


Fig. 5. Cyclic voltammograms of Pd/C and Pt@Pd/C catalyst electrodes measured at 2 M HCOOH in 0.5 M H₂SO₄ electrolyte at room temperature and with a sweep rate of 10 mV s⁻¹.

region (between 0 V and 0.1 V) where formic acid oxidation goes through the direct pathway. In contrast, the main oxidation peak for Pt/C was at 0.49 V, a position where CO pathway mechanism takes place [25]. The current density for Pt/C, Pd/C and Pt@Pd/C at 0.07 V is 1.1 mA cm⁻², 15.7 mA cm⁻² and 58.5 mA cm⁻² respectively. Monometallic Pt/C showed negligible activity at 0.07 V (the onset potential is also very positive, at 0.02 V). A very large current hysteresis loop (between the current measured in the positive and negative sweeps) is observed on monometallic Pt/C indicating significant poison. For comparison, the hysteresis loops for Pd/C and Pt@Pd/C catalysts are relatively small, suggesting a low poisoning rate. Obviously, the activity of Pt@Pd/C is threefold relative to that of the monometallic Pd/C catalyst. The CV shape of Pt@Pd/C demonstrated clearly synergetic effects of Pt and Pd. Moreover, the obvious oxidation peak at 0.72 V for Pt/C is completely suppressed on Pt@Pd/C catalyst indicating that the Pt surface is covered by Pd layer. The enhanced activity for Pt@Pd/C had to become from the unique core-shell structure since its S_{XRD} and ECSA are the smallest among all the catalysts.

Fig. 5 is the Pd mass normalized activity for Pd/C and Pt@Pd/C. At the peak current potential of the positive scan the activity of Pt@Pd/C is 3.9 A mg⁻¹Pd, whereas the activity for Pd/C is 1.2 A mg⁻¹Pd. The specific mass activity was increased more than fivefold at 0.1 V (0.74 A mg⁻¹ for Pd/C and 3.86 A mg⁻¹ for Pt@Pd/C). It should be noted that the particle size of Pd/C and Pt@Pd/C is 3.4 nm and 4.1 nm respectively.

4. Conclusions

Core-shell Pt@Pd/C catalyst was prepared by a two-step colloidal approach for application in formic acid oxidation. The structure of Pt@Pd/C is extensively characterized by XRD, TEM and XPS. Proven evidence for the core-shell structure of Pt@Pd/C was not found due to the similar crystal lattice of Pt and Pd. Nevertheless, the catalyst Pt@Pd/C showed a strong enhanced activity for the anodic formic acid compared with that of Pt/C and Pd/C catalysts making it a promising anodic catalyst for direct formic acid fuel cells.

Acknowledgments

We would like to thank the National Scientific Foundation of China (NSFC projects nos. 20673040, 20876062), the Ministry of Science and Technology of China (project no. 2009AA05Z119) and the Guangdong Provincial Scientific Foundation (project no. 36055) for financial support of this work.

References

- [1] X. Li, I.M. Hsing, *Electrochim. Acta* 51 (2006) 3477–3483.
- [2] C. Jung, C.M. Sainchez-Sainchez, C.-L. Lin, J.n. Rodriiguez-Loipez, A.J. Bard, *Anal. Chem.* 81 (2009) 7003–7008.
- [3] B. Liu, H.Y. Li, L. Die, X.H. Zhang, Z. Fan, J.H. Chen, *J. Power Sources* 186 (2009) 62–66.
- [4] J.L. Haan, R.I. Masel, *Electrochim. Acta* 54 (2009) 4073–4078.
- [5] Y. Wang, X. Wu, B. Wu, Y. Gao, *J. Power Sources* 189 (2009) 1020–1022.
- [6] Y. Huang, X. Zhou, J. Liao, C. Liu, T. Lu, W. Xing, *Electrochem. Commun.* 10 (2008) 1155–1157.
- [7] M.A. Rigsby, W.-P. Zhou, A. Lewera, H.T. Duong, P.S. Bagus, W. Jaegermann, R. Hunger, A. Wieckowski, *J. Phys. Chem. C* 112 (2008) 15595–15601.
- [8] X. Wang, Y. Tang, Y. Gao, T. Lu, *J. Power Sources* 175 (2008) 784–788.
- [9] J.Y. Wang, Y.-Y. Kang, H. Yang, W.-B. Cai, *J. Phys. Chem. C* 113 (2009) 8366–8372.
- [10] Z. Bai, L. Yang, L. Li, J. Lv, K. Wang, *J. Phys. Chem. C* 113 (2009) 10568–10573.
- [11] Y. Huang, X. Zhou, J. Liao, C. Liu, T. Lu, W. Xing, *Electrochem. Commun.* 10 (2008) 621–624.
- [12] Y. Zhu, Y. Kang, Z. Zou, Q. Zhou, J. Zheng, B. Xia, H. Yang, *Electrochem. Commun.* 10 (2008) 802–805.
- [13] L.R. Alden, C. Roychowdhury, F. Matsumoto, D.K. Han, V.B. Zeldovich, H.D. Abruna, F.J. DiSalvo, *Langmuir* 22 (2006) 10465–10471.
- [14] S.L. Gojković, A.V. Tripković, R.M. Stevanović, N.V. Krstajić, *Langmuir* 23 (2007) 12760–12764.
- [15] W. Liu, J. Huang, *J. Power Sources* 189 (2009) 1012–1015.
- [16] Z. Liu, X. Zhang, *Electrochem. Commun.* 11 (2009) 1667–1670.
- [17] D. Morales-Acosta, J. Ledesma-Garcia, L.A. Godinez, H.G. Rodriguez, L. Alvarez-Contreras, L.G. Arriaga, *J. Power Sources* 195 (2010) 461–465.
- [18] P. Waszczuk, T.M. Barnard, C. Rice, R.I. Masel, A. Wieckowski, *Electrochem. Commun.* 4 (2002) 599–603.
- [19] P.K. Babu, H.S. Kim, J.H. Chung, E. Oldfield, A. Wieckowski, *J. Phys. Chem. B* 108 (2004) 20228–20232.
- [20] J. Zeng, J. Yang, J.Y. Lee, W. Zhou, *J. Phys. Chem. C* 110 (2006) 24606–24611.
- [21] W. Zhou, J.Y. Lee, *Electrochem. Commun.* 9 (2007) 1725–1729.
- [22] Y.N. Wu, S.J. Liao, Z.X. Liang, L.J. Yang, R.F. Wang, *J. Power Sources* 194 (2009) 805–810.
- [23] W. Wang, D. Zheng, C. Du, Z. Zou, X. Zhang, B. Xia, H. Yang, D.L. Akins, *J. Power Sources* 167 (2007) 243–249.
- [24] B. Seger, A. Kongkanand, K. Vinodgopal, P.V. Kamat, *J. Electroanal. Chem.* 621 (2008) 198–204.
- [25] R. Wang, S. Liao, S. Ji, *J. Power Sources* 180 (2008) 205–208.